

Dorsal and ventral aspects of the most caudal medullary reticular formation have differential roles in modulation and formation of the respiratory motor pattern in rat

Sarah E. Jones¹ · Davor Stanić¹ · Mathias Dutschmann¹

Received: 6 August 2015 / Accepted: 26 November 2015 / Published online: 11 December 2015
© Springer-Verlag Berlin Heidelberg 2015

Abstract The respiratory pattern generator of mammals is anatomically organized in lateral respiratory columns (LRCs) within the brainstem. LRC compartments serve specific functions in respiratory pattern and rhythm generation. While the caudal medullary reticular formation (cMRF) has respiratory functions reportedly related to the mediation of expulsive respiratory reflexes, it remains unclear whether neurons of the cMRF functionally belong to the LRC. In the present study we specifically investigated the respiratory functions of the cMRF. Tract tracing shows that the cMRF has substantial connectivity with key compartments of the LRC, particularly the parafacial respiratory group and the Kölliker-Fuse nuclei. These neurons have a loose topography and are located in the ventral and dorsal cMRF. Systematic mapping of the cMRF with glutamate stimulation revealed potent respiratory modulation of the respiratory motor pattern from both dorsal and ventral injection sites. Pharmacological inhibition of the cMRF with the GABA-receptor agonist isoguvacine produced significant and robust changes to the baseline respiratory motor pattern (decreased laryngeal post-inspiratory and abdominal expiratory motor activity, delayed inspiratory off-switch and increased respiratory frequency) after dorsal cMRF injection, while ventral

injections had no effect. The present data indicate that the ventral cMRF is not an integral part of the respiratory pattern generator and merely serves as a relay for sensory and/or higher command-related modulation of respiration. On the contrary, the dorsal aspect of the cMRF clearly has a functional role in respiratory pattern formation. These findings revive the largely abandoned concept of a dorsal respiratory group that contributes to the generation of the respiratory motor pattern.

Keywords Respiratory pattern generation · Nucleus retroambiguus · Modulation of breathing · Cough · Sneeze

Introduction

Two bilateral columns of neurons stretching from the caudal ventrolateral medulla to the dorsolateral pons generate the mammalian breathing rhythm and respiratory motor pattern. The bilateral lateral respiratory columns (LRCs) are further subdivided into functionally (Smith et al. 2013), genetically (Gray 2013) and anatomically (Alheid et al. 2004) distinct compartments and sub-nuclei. Synaptic interactions within or between compartments of the LRC have specific roles in the generation of the sequential three-phase respiratory motor pattern of inspiration, post-inspiration (early expiration) and active expiration. The pre-Bötzinger complex (pre-BötC) initiates and generates inspiration (Feldman et al. 2013; Ramirez et al. 2012; Smith et al. 1991), while the generation of the subsequent post-inspiratory phase of the respiratory cycle depends on the synaptic interaction between the pontine Kölliker-Fuse nucleus (KF) and the medullary Bötzing complex (Burke et al. 2010; Dutschmann and Dick 2012; Dutschmann and Herbert 2006; Rybak et al. 2007; Smith

Electronic supplementary material The online version of this article (doi:10.1007/s00429-015-1165-x) contains supplementary material, which is available to authorized users.

✉ Mathias Dutschmann
mathias.dutschmann@floreys.edu.au

¹ Howard Florey Laboratories, Systems Neurophysiology Division, Florey Institute of Neuroscience and Mental Health, Gate 11 Royal Parade, University of Melbourne, Parkville, VIC 3010, Australia

et al. 2007). Active expiration, the last phase of the respiratory cycle, is always present centrally. However, its expression at the peripheral motor level (e.g., iliohypogastric nerve lumbar spinal cord) is variable (Abdala et al. 2009; Bautista and Dutschmann 2015; Iizuka and Fregosi 2007). Abdominal expiratory activity in last third of the respiratory cycle is reported to occur under high metabolic demand (e.g., exercise) or critical metabolic conditions such as hypoxia or hypercapnia, but is also present in baseline respiratory motor patterns of the perfused brainstem preparation (Abdala et al. 2009; Bautista and Dutschmann 2015; Farmer et al. 2014; Zoccal et al. 2008). The generation of late expiratory activity is associated with the parafacial respiratory group and retrotrapezoid nucleus pFRG/RTN of the caudal pons (Guyenet 2012; Janczewski and Feldman 2006; Onimaru and Homma 2003).

The functions of the previously mentioned key areas of the LRC are well established. However, nuclei of the most caudal medullary reticular formation (cMRF), such as the nucleus retroambiguus [NRA; (Olszewski 1954)] received less research attention. The major function of the NRA is seen in generation (Janczewski et al. 2002) and modulation of active expiration (Boers et al. 2006; Merrill 1974; Subramanian and Holstege 2009). Moreover, it is reported that the NRA can facilitate a variety of expiratory-related reflexes and behaviors such as coughing, sneezing, vomiting and also vocalization in which increased intra-abdominal and or intrathoracic pressure is required (Cinelli et al. 2012; Gestreau et al. 1997; Jakus et al. 1985; Miller et al. 1987; Mutolo et al. 1985; Nonaka and Miller 1991; Oku et al. 1994; Poliacsek et al. 1985; Subramanian and Holstege 2009; Sugiyama et al. 2010; Wallois et al. 1992). Compared to other areas of the LRC the role of the cMRF in respiratory rhythm generation and formation of the three-phase motor pattern remains controversial. The identification of the pre-BötC as the rhythmogenic kernel (Smith et al. 1991) for respiration diminished the interest in the function of the caudal medullary areas. The ventral cMRF is often presented as part of LRC (Alheid et al. 2004; Rybak et al. 2007; Smith et al. 2013; Smith et al. 2009), however, its role in respiratory rhythm and pattern generation has only been sporadically investigated (Jones et al. 2012; McCrimmon et al. 2000a; Merrill 1970; Merrill 1974; Monnier et al. 2003; Oku et al. 2008). Another reason for lack of research focus on these caudal areas is due to the fact that rodents, as the main experimental animal model for control of breathing, neither cough (Ohi et al. 2004) nor vomit (Borison et al. 1981). Thus the cMRF, including the NRA, appears to be less relevant for respiratory control and modulation in these species.

In light of recent studies from our laboratory that suggested potential rhythm promoting mechanisms of the cMRF in rat (Jones et al. 2012), we systematically

investigated its ascending synaptic connectivity with primary nuclei of the LRC and its respiratory functions. The current study aimed to elucidate the role and contribution of the cMRF in the generation of respiratory rhythm and or the modulation of the respiratory motor pattern. Our data show that the cMRF has significant connectivity with key nuclei of LRC. Tract tracing experiments identify a dorsal and ventral (overlapping with the NRA) cluster of projection neurons. Glutamate micro-stimulation of either aspect of the cMRF triggered a variety of respiratory modulations, while local circuitry inhibition revealed that only the dorsal cluster of projection neurons has a role in the generation of the basic respiratory motor pattern.

Materials and methods

Sprague–Dawley rats were maintained on a 12 h light/dark cycle with food and water available ad libitum. All experiments followed protocols approved by the Florey Institute of Neuroscience and Mental Health Animal Ethics Committee (AEC 12-005), and performed in accordance with the NHMRC Code of Practice for the Use of Animals for Scientific Purposes.

Anesthesia for anatomical tract tracing experiments

Rats of either sex were used for the tracer experiments. Animals were initially sedated with diazepam (5 mg/kg i.m.) and anaesthetized 10 min later with ketamine (100 mg/kg i.p.).

Tracer substances: Three different anatomical tracers were used. All anterograde tracing experiments used 10 % biotinylated dextran amine (NeuroTrace, Molecular Probes, OR, USA) with injection volumes of 80 nL. Retrograde tracing experiments were performed using 2 % Fast Blue (Polysciences Inc, PA, USA) or Cholera toxin subunit B (CTb) conjugated to Alexa Fluor 488 (1 mg/mL; Invitrogen, OR, USA) with injection volumes of 80 nL. All microinjections were performed using a calibrated borosilicate glass micropipette and were pressure induced.

Anterograde tracer injections into cMRF

Rats were secured in stereotaxic apparatus (TSE Systems, Bad Homburg, Germany) at interaural zero. A midline incision was made from the occipital bone running 2 cm caudal through the skin and superficial muscle layer. Deep neck muscles were parted at the midline to expose the cisterna magnum and the atlanto-occipital membrane was cut away to expose the 4th ventricle at the level of the obex. Positioning of the stereotaxic nose bar was adjusted to flex the skull 90° downward from interaural zero,

bringing the brainstem into the horizontal plane. Microinjections targeted into cMRF ($n = 10$) were made 1.1 mm caudal to obex, 1.3 mm lateral to midline and 1.2 mm ventral from the dorsal brain surface. Following the microinjection, the micropipette remained in position for 10 min to minimize backflow. Injection volumes were controlled via movement of the fluid meniscus along a calibrated tube used for the pressure microinjections.

Retrograde tracer injection into selected compartments of the LRC

Microinjections targeted into the VRG ($n = 11$) used the same surgical approach as described for the NRA. Microinjections were made at coordinates 1.2 mm caudal to obex, 2 mm lateral to the midline and 3.2 mm ventral to dorsal surface of the brain. The injecting micropipette was angled 36° forward from vertical, facilitating access to rostral areas of the medulla oblongata.

For retrograde tracer injection into the retromedial nucleus/parafacial respiratory group (RTN/pFRG) and Kölliker-Fuse (KF) nucleus, rats were secured in a stereotaxic apparatus at interaural zero and a midline incision was made to expose the skull from bregma to lambda. A burr hole was drilled through the skull and tracer injections into the RTN/pFRG ($n = 18$) were made 6.5 mm caudal to bregma and 2.1 mm lateral to midline. The pipette was angled 25° backwards from vertical, and the final injections were made 11.2 mm ventral to the dorsal brain surface. KF injections ($n = 21$) were made at 9.0 mm caudal to bregma, 2.5 mm lateral to midline and 6.8 mm ventral to the dorsal brain surface. Following all microinjections the micropipette remained in position for 10 min to minimize backflow, and removed at a rate of 1 mm/min.

Tissue processing

7–10 days after tracer injections, animals were anaesthetized with a terminal overdose of sodium pentobarbital (90 mg/kg i.p.) and perfused transcardially with 100 ml Tyrode's buffer (pH 7.4), followed by 300 ml of 0.16 M phosphate buffer (pH 7.35) containing 4 % paraformaldehyde and 0.2 % picric acid. The brain and spinal cord up to cervical segment 2 were then dissected, post-fixed for 90 min and transferred to 0.1 M phosphate buffer (pH 7.4) containing 10 % sucrose for 2 days. Brains were frozen using compressed CO₂ and 40 µm free-floating sections cut serially using a cryostat (Leica Biosystems, IL, USA).

Anterograde tracer experiments: Sections were incubated in 1.0 µg/ml avidin–horseradish peroxidase (Molecular probes, Life technologies, OR, USA #N-7167) overnight at 4 °C, washed in 0.1 M PBS and immersed in diaminobenzidine (DAB) substrate (1:10, Roche

Diagnostics, Mannheim, Germany) for 30 min allowing visualization of the tracer via a stable fade-resistant dark brown reaction product. Sections were then counterstained using 0.25 % cresyl violet (Sigma-Aldrich), rinsed in graded ethanol solutions, and coverslipped with DPX (Sigma-Aldrich).

Retrograde tracer experiments: CTb was pre-conjugated to Alexa Fluor 488 and was visible under fluorescence microscopy. However, in order to enhance visibility of retrogradely labeled soma additional immunohistochemistry was performed. For optimum visualization of CTb, sections were incubated overnight at RT with a goat anti-CTb antibody (1:10,000 List Biological Laboratories, CA, USA) diluted in 0.1 M PBS containing 0.3 % Triton X-100 and 0.5 % BSA. Sections were then washed (0.1 M PBS, 3 × 20 min), blocked (5 % normal donkey serum in 0.1 M PBS for 1 h), and incubated in donkey anti-goat-Alexa 488 (1:200, Jackson ImmunoResearch, PA, USA) for 2 h before being washed, mounted onto gelatin coated slides, and coverslipped with a fluorescent anti-fade mounting medium (Fluoroshield, Sigma Aldrich, MO, USA). A rabbit anti-tyrosine hydroxylase antibody (1:500, Pel-Freez Biologicals, AR, USA; Code No. p40101-0) was added together with CTb antibody, and visualized using donkey anti-rabbit-Alexa 594 (1:200, Jackson ImmunoResearch). Sections from animals that received fast blue injections were coverslipped using the same mounting medium.

Data analysis: tract tracing

Ipsilateral counts of retrogradely labelled cell bodies were made using Stereoinvestigator v7.0 software (MBF Bioscience, VT, USA). Cell bodies were viewed using a microscope and ×63 oil objective (Leica Biosystems), and every 6th section was examined. Neuronal plots of retrogradely labelled cells from representative microinjections were made from photomicrographs taken using a ×10 objective. The labeled somata were then superimposed over schematic diagrams and represented as dots.

Anterograde labelling of nerve terminal fields was assessed using semi-quantitative comparative analyses, with the relative abundance of labelled nerve fibres, boutons and varicosities evaluated on a five point scale: (–) absence of labelled terminals; (±) very low density; (+) low density; (++) moderate density; (+++) high density. Assessment was comparative, and the illustrative examples of different densities used for assessment are included in Fig. 2.

Working heart brainstem preparation

Experiments were performed using the in situ perfused brainstem-spinal cord preparation of juvenile Sprague–

Dawley rats aged post-natal day 18–23 ($n = 62$). Basic procedures were performed in accordance with previously published studies (Paton 1996; Dutschmann et al. 2009). In short, rats were deeply anaesthetized via inhalation of isoflurane until complete loss of the hindpaw withdrawal reflex in response to a noxious pinch. They were rapidly bisected below the diaphragm and decerebrated at the pre-collicular level. The cerebellum, occipital bone and atlas bone were removed for optimum visualization of the dorsal, caudal brainstem surface. The right thoracic phrenic nerve and right cervical vagus nerve were isolated and cut distally. Additionally, in a subset of experiments, the iliohypogastric branch of the abdominal nerve was isolated. The descending aorta was cannulated and perfused retrogradely with carbogenated Ringer solution (31 °C) using a peristaltic pump (Watson and Marlow, Stockholm, Sweden) in order to elicit a consistent eupneic respiratory motor discharge, obtained at flow rates of 18–22 mL/min, relating to a perfusion pressure of 40–70 mmHg.

Nerve recordings

Nerve activity was recorded from cut proximal nerve ends using suction electrodes; signals were amplified (differential amplifier DP-311, Warner instruments, Hamden, USA), band-pass filtered from 100 to 5 kHz, digitized (PowerLab/16SP ADInstruments, Sydney Australia) and then viewed and recorded on LabChart v7.0 software (ADInstruments). Additional post hoc analysis included applying a high pass digital filter at a cut off frequency of 20 Hz to stabilize the baseline recording and eliminate movement artifacts.

Microinjections

Pressure-induced microinjections of 50 nL were performed using calibrated borosilicate glass micropipettes.

Multi-barrel pipettes were used, including a barrel containing Chicago sky blue (2 %) or rhodamine beads, a barrel containing 10 mM L-glutamate, and a barrel containing an inhibitory pharmacological agent 10 mM isoguvacine (or 2 M glycine, or a 1:1 mixture of 10 mM isoguvacine and 2 M glycine—detailed results not presented). Microinjections of glutamate were given in a 48 point grid. Injection coordinates were measured from obex, a landmark clearly visible on the dorsal brainstem surface. Injections were made 400 μ m apart, with most rostro-caudal coordinates at 0.8, 1.2, 1.6 and 2.0 mm caudal to obex, lateral coordinates at 1.2, 1.6 and 2.0 mm lateral to midline, and 0.6, 1.0, 1.4 and 1.8 mm ventral to the dorsal surface. When a notable response was elicited at a stimulation site, the site was marked with the Chicago sky blue or rhodamine beads. A maximum of two injection sites were marked per animal to ensure correct histological

identification and verification of relevant sites. Marking two injection sites per brainstem allowed retrospective anatomical verification of injection sites within the pre-designed grid and importantly the extrapolation of additional unmarked injection sites. This ensured an accurate reconstruction of the injection grid and response topography. Inhibitory microinjections (Isoguvacine/glycine) were concentrated over stimulation sites prone to eliciting a strong tachypneic or strong post-inspiratory modulatory respiratory effect. Once injections were complete, brains were removed and post-fixed in 4 % paraformaldehyde for 3 days before being transferred to 0.1 M phosphate buffer containing 10 % sucrose for 2 days and 50 μ m sections sliced using a cryostat (Leica Biosystems). Sections were mounted and counterstained with 1 % Neutral Red (Sigma-Aldrich) in order to validate anatomical location of injection sites.

Data analyses

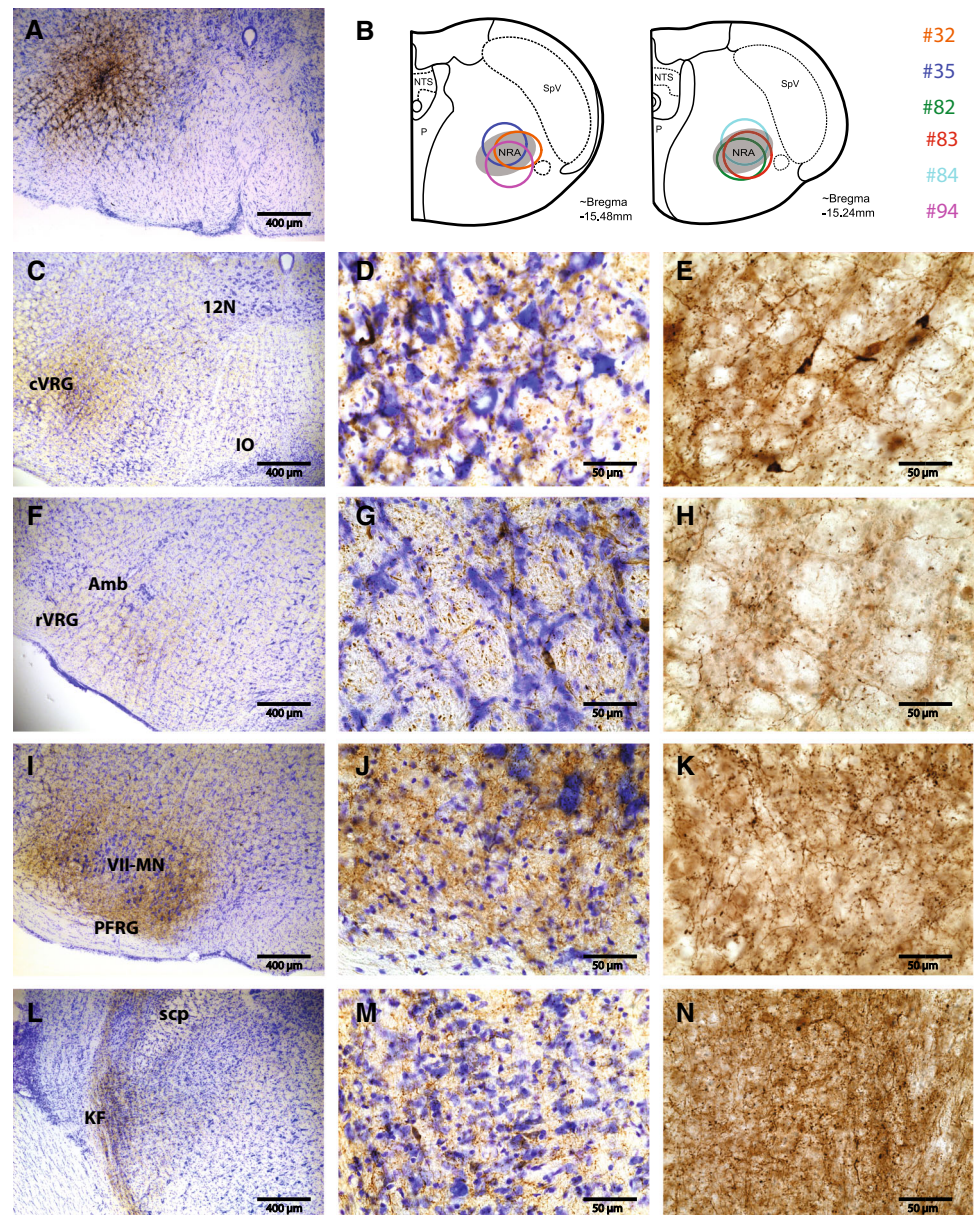
Analysis of respiratory motor activity was performed with LabChart v7.0 software (ADInstruments, Dunedin, New Zealand). In order to analyze respiratory motor pattern and frequency changes in response to isoguvacine, respiratory parameters including duration of inspiration (T_i), post-inspiration (T_{pi}) and total respiratory cycle duration (T_{tot}) were measured over a 60 s period before, and 2 min after, effective drug injection. The same protocol was used for the analysis of arterial chemoreceptor evoked respiratory responses. In addition, we plotted the instantaneous T_{tot} to illustrate the dynamic changes in respiratory frequency (Fig. 8). Statistical tests were performed with paired Student t tests and a value of $p \leq 0.05$ was considered statistically significant. Values are expressed as the mean \pm SEM.

Results

Ascending projection of the cMRF targeting the lateral respiratory column of the brainstem

Injections (80 nL) of the anterograde tracer biotinylated dextran amine were made into the cMRF 0.8–2 mm caudal to obex. In 6/10 experiments the injection sites were located in the ventral cMRF, overlapping with the NRA (Fig. 1a, b, Exp. 32, 35, 82–84, 94). In all of these cases, ascending terminal fields were observed across the entire rostro-caudal extension of the brainstem LRC. The density of labeled axon terminals (e.g. varicosities) in the medullary aspects of the LRC showed a caudal-rostral gradient. The caudal and rostral ventral respiratory group (VRG) showed dense terminal fields (see Fig. 1c–e), while more

Fig. 1 Color photomicrographs of anterogradely labeled neuron terminals following injection of biotinylated dextran amine into the ventral caudal reticular formation overlapping with nucleus retroambiguus. Sections in the first and second columns are counterstained with cresyl-violet, and the last column shows the same anatomical area from an adjacent section, without counterstain. **a** Coronal section of the caudal medulla at the level of the pyramidal decussation, a representative example (experiment #83) of injection site and spread of biotinylated dextran amine (brown) overlapping with nucleus retroambiguus. Location of additional injection sites not photographed are displayed in **(b)**. Anterogradely labeled neuronal axons, terminals and boutons (brown) ipsilateral to injection site were seen in clusters in the: **c–e** caudal ventral respiratory group (c-VRC); **f–h** rostral ventral respiratory group (r-VRC); **i–k** parafacial respiratory group/retrotrapezoid nucleus (pFRG/RTN) and lateral aspects of the facial motor nucleus (7); and in **l–n** the Kölliker-Fuse nucleus (KF)



rostral medullary nuclei such as the pre-BötC and BötC received less dense innervation from the cMRF. In addition to medullary projections, dense terminals were detected in pontine aspects of the LRC. The densest labeling was observed at the caudal and rostral poles of the pontine LRC. At the level of the caudal pons, dense terminals were seen in the pFRG/RTN region (Fig. 1i–k). In the rostral pons, specific and dense nerve terminals were seen in the KF nucleus (Fig. 1l–n). Terminal fields were also consistently observed caudal and ventral to the KF nucleus in areas that are defined as the inter-trigeminal region of the LRC. Finally, the A5 region, which is also part of the LRC, contained a medium density of labeling. Across the $n = 6$ examples the relative proportions of observed terminal

fields were consistent, although mild variation in terminal field density was observed between cases, likely due to inevitable variation in injection spread and uptake at the nucleus retroambiguus. The terminal fields observed within the full extension of ponto-medullary LRC showed a strong ipsilateral predominance. Contralateral terminals were seen in all analyzed nuclei (see Fig. 2).

Terminal fields in brainstem motor nuclei and nuclei outside the lateral respiratory column

In addition to the terminal fields in the LRC, respiratory motor nuclei received innervation from the cMRF. The densest innervation was observed in lateral columns of the

	Ipsilateral	Contralateral
A		
Medulla		
vINTS	+	±
cNTS	-	-
dmNTS	-	-
Mo12	+	±
cVRG	+++	++
rVRG	+	±
Pre-BötC	++	+
Böt	+	±
Mo7	+++	+
Raphe	-	-
Pons		
Mo5	+	-
pFRG/RTN	+++	+
KF	+++	+
Midbrain		
vlPAG	+	-
IPAG	-	-
dmPAG	±	-

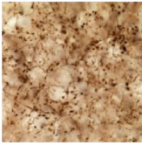
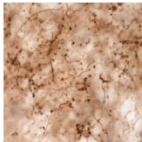
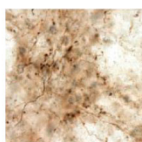

B		+++ Example from pFRG/RTN
		++ Example from pre-BotC
		+ Example from rVRG
		+ Example from dmPAG

Fig. 2 a Table depicting ipsilateral and contralateral densities of biotinylated dextran amine (BDA) labelled fibres, boutons and varicosities following microinjection of BDA into the nucleus retroambiguus. Density was evaluated on a five point scale: (–) absence of labelled terminals; (±) very low density; (+) low density; (++) moderate density; (+++) high density. **b** 100 μm^2 representative example images depicting each density level. Ventrolateral nucleus of the solitary tract (vINTS), commissural nucleus of the solitary tract (cNTS), dorsomedial nucleus of the solitary tract

(dmNTS), hypoglossal motor nucleus (Mo12), caudal ventral respiratory group (cVRG), rostral ventral respiratory group (rVRG), pre-Bötzinger complex (pre-BötC), Bötzinger complex (Böt), facial motor nucleus (Mo7), trigeminal motor nucleus (Mo5), parafacial respiratory group/retrotrapezoid nucleus (pFRG/RTN), Kölliker Fuse nucleus (KF), ventrolateral periaqueductal gray (vlPAG), lateral periaqueductal gray (IPAG) and dorsomedial periaqueductal gray (dmPAG)

facial motor nucleus (Fig. 1i) and the terminal fields within VRG overlapped with the laryngeal motor neurons located within the loose formation of the nucleus ambiguus (see Fig. 1f). Innervation of the hypoglossal and trigeminal motor nuclei, however, was modest. Low-density terminal fields were also observed in the nucleus of the solitary tract (NTS) but were restricted to the ventrolateral subnuclei. In the midbrain, modest labeling was observed in the lateral and ventrolateral columns of the periaqueductal gray. Finally, no terminals were detected in the midline raphe nuclei after anterograde tracer injection into the cMRF.

Retrograde labeling of cMRF neurons projecting into selected nuclei of the LRC

Microinjections of the retrograde tracers fast blue or CTb (80 nL) were made into the VRG ($n = 11$), the pFRG/RTN ($n = 18$) and the KF ($n = 21$) since these LRC target areas showed the most dense terminal fields in the anterograde tracing experiments. Photos of injection sites within the VRG, pFRG/RTN and KF and the corresponding pools of retrogradely labeled cells in the dorsal caudal medulla and

NRA are illustrated in Fig. 3. Immunohistochemistry for tyrosine hydroxylase shows that the retrogradely labeled cells do not overlap with the noradrenergic A1 and A2 cell populations.

Detailed plots of the location and cell counts of retrogradely labeled cells at various levels of the caudal medulla are shown in Figs. 4 and 5. Retrograde tracer injections that were successfully delivered into all three target areas showed a relatively uniform pattern of a ventral and dorsal cluster of labeled neurons in the lateral caudal medulla, illustrated in representative examples in Fig. 4. No specific cell markers (e.g., developmental transcription factors, neuropeptides) for these two clusters of neurons are currently identified and thus the clusters are characterized merely on their anatomical location. Subsequent physiology experiments (described later) strongly support the notion of two distinct neuronal populations that have different respiratory function, although sharing common ascending targets within the LRC. Additionally, irrespective of the target area all retrograde tracer injections also labeled cells within the NTS, (see Fig. 4). In accordance with the literature, NTS labeling was most dense following

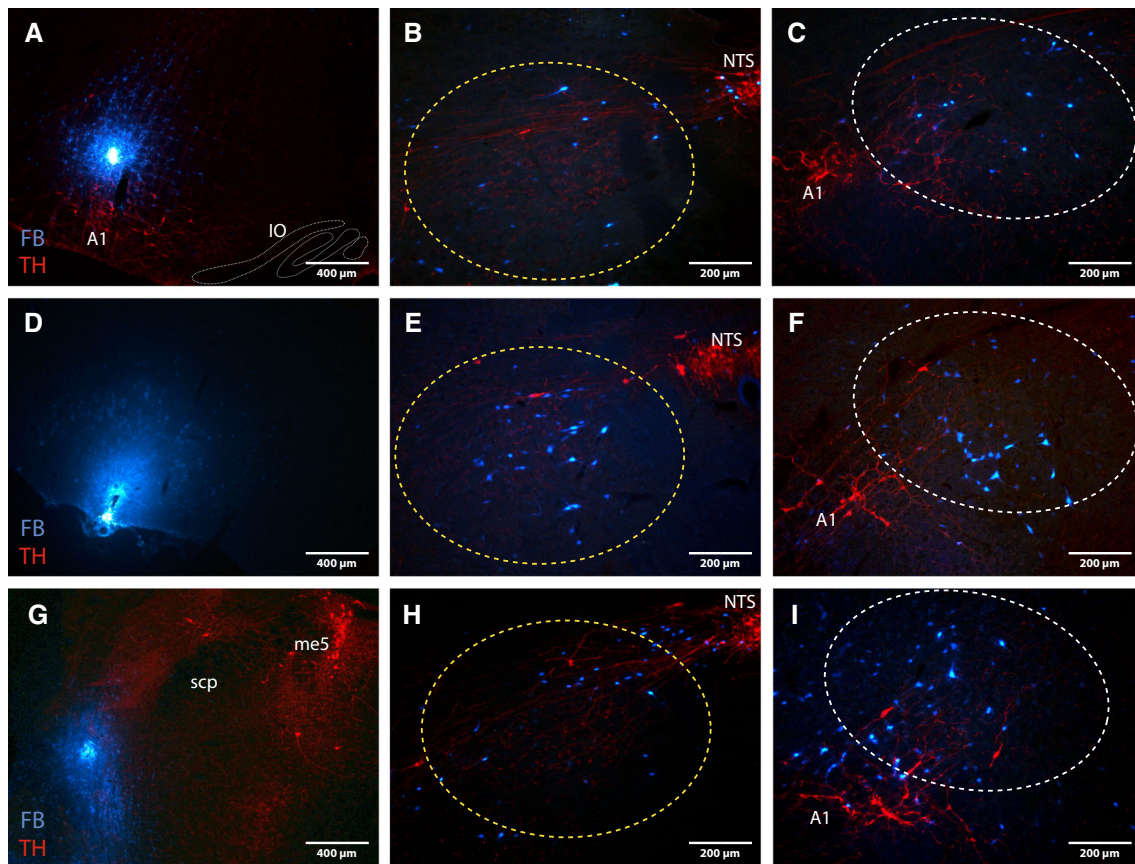


Fig. 3 Color photomicrographs of Fast-blue (FB) retrogradely labeled neurons (blue) and tyrosine hydroxylase (TH) staining of adrenergic A1 and A2 cell populations (red) as anatomical landmarks. Retrogradely labeled cells are imaged at two areas of interest, both at the rostro-caudal level of the pyramidal decussation; the dorsal

respiratory group, DRG (yellow circles) and nucleus retroambiguus, NRA region (white circles) as labeled from tracer injections into **a–c**: ventral respiratory group, VRC, **d–f**: parafacial respiratory group, pFRG/RTN and **g–i**: Kölliker-Fuse nucleus, KF

retrograde tracer injection into the pFRG/RTN and KF (Herbert et al. 1990; Rosin et al. 2006). Somata of projection neurons within the caudal nucleus of the spinal trigeminal tract (Sp5) were also observed, but only after injections into the KF, in accordance with previous literature (Feil and Herbert 1995).

Quantification of the dorsal and ventral (NRA) clusters of retrogradely labeled neurons was performed in cases of successful tracer injections ($n = 4$ for each of the three target areas).

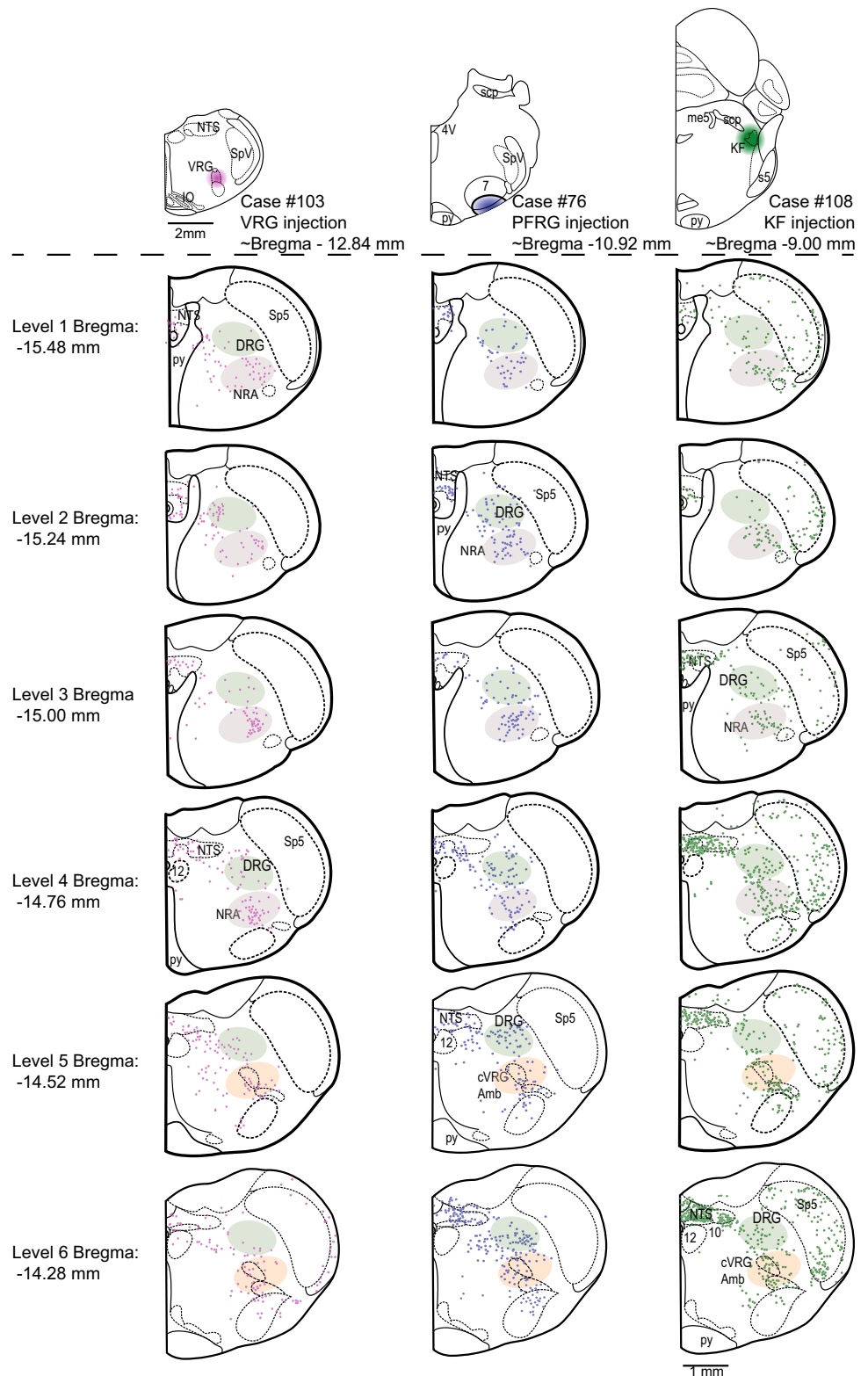
The number of retrogradely labeled projecting neurons in the ventral cMRF, overlapping with the NRA, was quantified from sections ranging from -15.48 to -14.76 mm relative to Bregma (Paxinos and Watson 2007). The cMRF/NRA contained 226 ± 24 , 223 ± 19 and 165 ± 9 cell bodies following injections derived from the KF, pFRG/RTN and VRG, respectively, and no statistical difference was found. Following a similar pattern, the dorsal cMRF contained 277 ± 14 , 283 ± 15 and 194 ± 29 cell bodies after injections into the KF, pFRG/

RTN and VRG, respectively, with the numbers of cells observed being statistically similar, see Fig. 5.

Mapping the caudal medulla for glutamate evoked respiratory responses

Microinjections of L-glutamate (50 nL) into the cMRF were performed in a total of 19 in situ preparations. We mapped the cMRF with $n = 379$ discrete glutamate microinjections following a 48 point grid. Microinjections triggered modulations in the respiratory pattern in $n = 269/379$ cases. The majority of the respiratory changes were associated with changes to the baseline respiratory frequency with $n = 110$ injections evoking tachypnea and $n = 98$ evoking a bradypnea. A further $n = 61$ glutamate microinjections evoked a brief modulation of respiratory motor pattern, amplitude or abdominal nerve activation, without a concurrent modulation of the respiratory rate. Finally, $n = 110$ glutamate microinjections were ineffective, causing no respiratory modulation. The glutamate mapping did not uncover

Fig. 4 Line drawings showing the distribution of ipsilateral retrogradely labeled neurons (colored dots) following injection of retrograde tracer into: **a** ventral respiratory group (VRG), **b** parafacial respiratory group (pFRG/RTN), and **c** Kölliker Fuse nucleus (KF). The grey shaded area represents the region of the reticular formation pertaining to the nucleus retroambiguus (NRA), and the pale orange shading marks the transitional region from NRA to nucleus ambiguus (Amb). The pale green shaded area represents the dorsal respiratory group (DRG) distinct from the nucleus of the solitary tract (NTS). Each line drawing represents the information of a 40 μm coronal brain section, with one dot plotted per somata as viewed under a $\times 10$ objective. Every 6th section was analyzed serially, with intervals of 240 μm . Levels caudal to Bregma on the left hand side are given as an approximate guide relating to the Rat Brain Atlas (Paxinos and Watson 2007)



a topographical organization of respiratory responses across the rostral caudal axis (suppl. Figure 1) and respiratory modulations were triggered from the dorsal reticular

formation as well as from the ventral NRA region. Figure 6 shows a variety of glutamate evoked respiratory modulations from both dorsal and ventral injection sites. Figure 6a shows

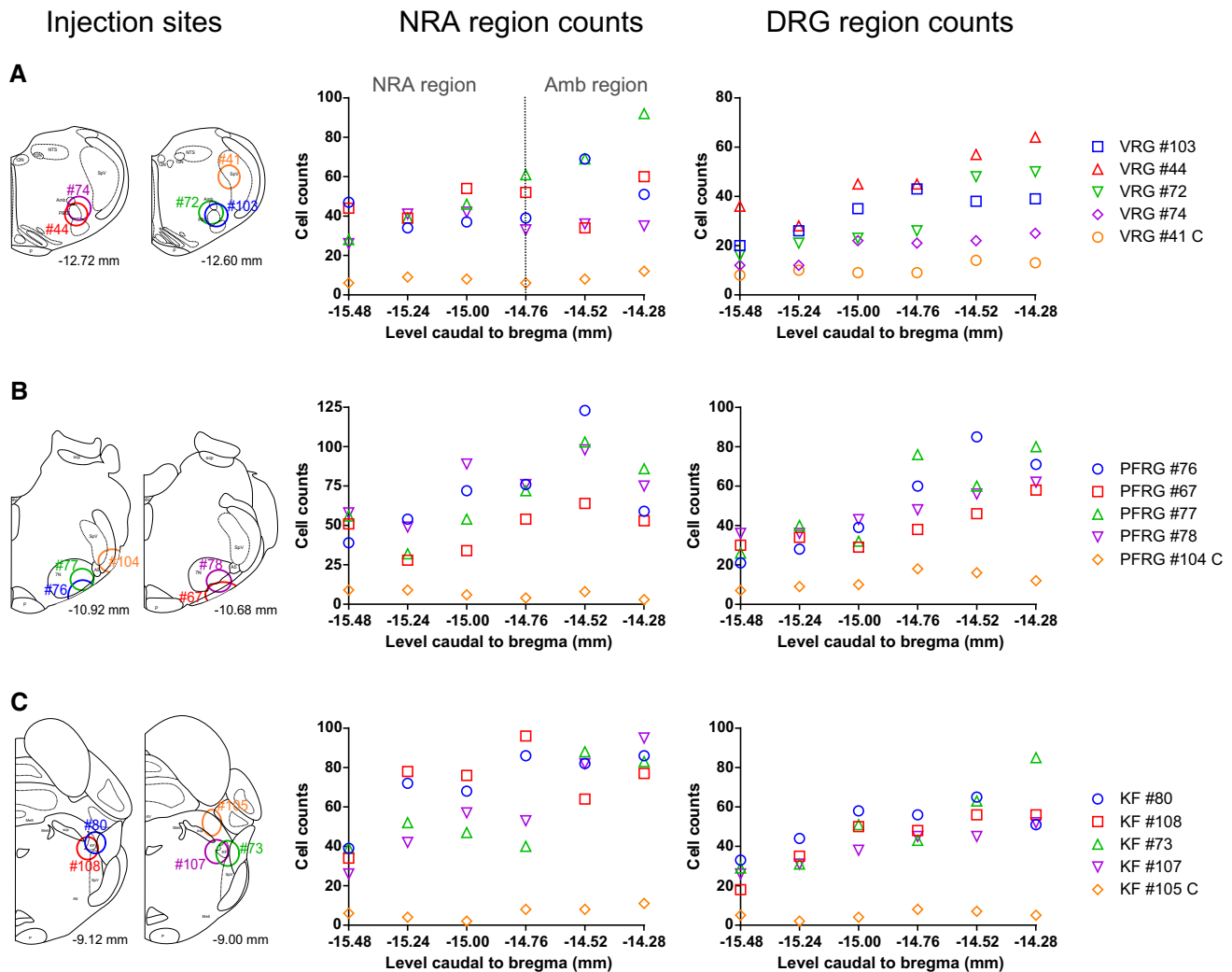


Fig. 5 Cell counts of retrogradely labeled somata in the nucleus retroambiguus region (NRA) and dorsal respiratory group (DRG) following retrograde tracer injections into the: **a** ventral respiratory group (VRG); **b** parafacial respiratory group/retrotrapezoid nucleus (pFRG/RTN); and **c** Kölliker-Fuse nucleus (KF). Counts are plotted against their rostro-caudal brain position [using (Paxinos and Watson

2007) as a guide]. Counts were made in five animals per injection target, with four injections hitting the target and one control injection site, which did not overlap target nucleus (*orange*). Locations of injection sites for each case are represented on the schematic drawings on the *left hand side*

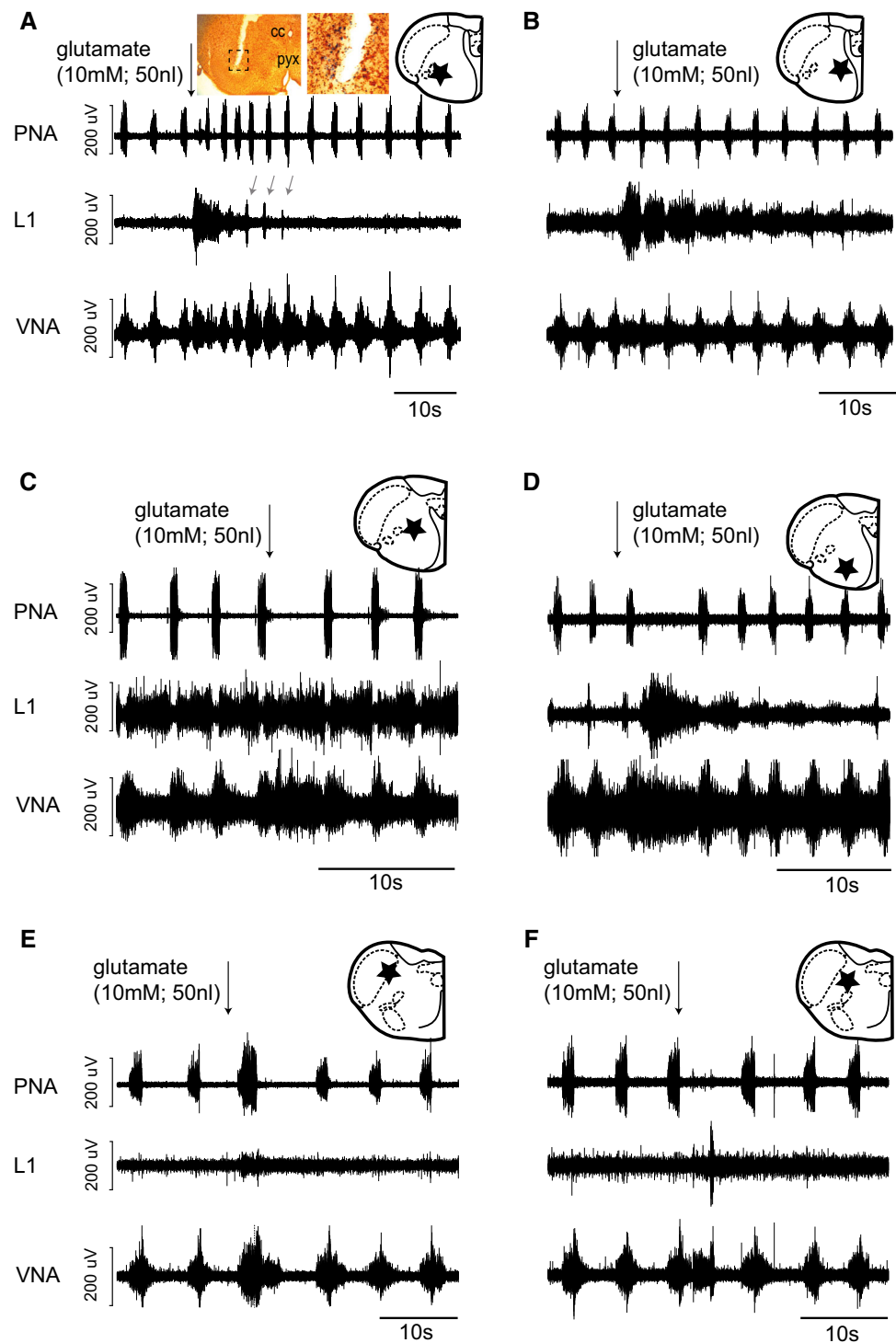
an evoked tachypneic response that involved a reduction in T_i , transient increase in PNA amplitude and enhanced abdominal expiratory activity in the iliohypogastric nerve recordings (L1). In this example VNA was modulated differentially. In the initial phase of the glutamate response, post-inspiratory discharge was reduced while later, a pronounced increase in both inspiratory and post-inspiratory activity can be observed. Figure 6b shows an example where glutamate evoked no change in PNA burst frequency but reduced T_i and triggered a prominent activation of abdominal expiratory activity during the expiratory intervals. Panels C and D of Fig. 6 show examples of glutamate evoked prolongation of expiration. The expiratory lengthening was usually associated with increased post-inspiratory activity in

the VNA that was accompanied by pronounced activation of abdominal expiratory activity in iliohypogastric nerve recordings. Finally panels E and F illustrate brief glutamate evoked respiratory events such as augmented breath (E) or enhanced post-inspiratory and abdominal expiratory activities that did not reset the respiratory cycle (i.e. there was no change in respiratory frequency) (F).

Changes in the baseline respiratory motor pattern following pharmacological inhibition of the dorsal and ventral cMRF

Sites at which robust respiratory modulation had been seen in response to injection of glutamate subsequently received

Fig. 6 Glutamate microinjection into the caudal medulla evoked a range of respiratory modulations. Shown are a variety of representative traces with photographic and schematic presentation of microinjection location. **a** glutamate evoked tachypnea associated with a decrease in T_i , transient PNA amplitude increase and activation of the iliohypogastric nerve (L1). **b** activation of iliohypogastric nerve activity and decreased T_i in absence of change to respiratory frequency. **c** and **d** Prolongation of expiration associated with increase in P_i duration and concurrent iliohypogastric nerve activation. **e** Augmented breath with modest iliohypogastric activation. **f** Augmented expiration, with enhanced P_i and late expiratory activation in the iliohypogastric nerve



small volumes (50 nL) of the GABA A receptor agonist isoguvacine ($n = 20$ preparations).

Isoguvacine microinjections made ventrally, from 1.2 to 1.8 mm ventral to the dorsal surface of the brain ($n = 15$), had no significant effects on the baseline respiratory motor pattern or rate, despite the robust glutamate evoked respiratory modulations that were observed at the same loci.

The lack of effect on the baseline respiratory motor pattern after NRA inhibition was further verified by $n = 2$ microinjections of the inhibitory amino acid glycine (2 M) or injection of a mix of 10 mM isoguvacine and 2 M glycine ($n = 5$). Neither glycine nor the isoguvacine and glycine mix evoked any change in the baseline motor pattern or frequency of respiration.

In order to elucidate a potential role of the dorsal cMRF and NRA in the mediation of changes of respiratory motor pattern during periods of increased chemical drive, we analyzed the expression of the sodium cyanide (NaCN) evoked arterial chemoreceptor before and after NRA inhibition ($n = 5$ preparations). NRA inhibition had no effect on the acute phase of the arterial chemoreceptor reflex-mediated respiratory augmentation, or on the post-stimulus period of enhanced late expiratory activity in the iliohypogastric nerve recording (see Fig. 8).

Contrary, microinjections of isoguvacine made dorsal to the NRA region, approximately 1.5 mm caudal to obex and 0.6–1.2 mm ventral to the dorsal brain surface ($n = 13$), triggered a modest but consistent and significant modulation of the baseline respiratory motor pattern. T_i increased on average 18 % from 0.91 ± 0.06 to 1.08 ± 0.06 s ($p = 0.004$), while T_{pi} decreased on average by 32 % from 2.70 ± 0.3 to 1.9 ± 0.40 s ($p = 0.003$). The overall respiratory frequency increased on average 20 % from 15.3 ± 1.5 bpm at baseline to 18.3 ± 1.9 bpm ($p = 0.009$) following isoguvacine microinjection. In 7/13 preparations, iliohypogastric nerve (L1 see Fig. 7) discharge could be analyzed because the recording had clear expiratory activity during conditions of baseline respiration in situ. In these experiments, isoguvacine injections reduced in the amplitude of the late expiratory abdominal nerve activity of on average 42.4 %, from a baseline of 220.3 ± 70.0 to 126.6 ± 35.0 μ V ($p < 0.05$). In four out of the seven preparations, low amplitude bursts during the post-inspiratory phase (early expiration) were visible. In all cases isoguvacine injection into the dorsal cMRF completely abolished the post-inspiratory activity of the iliohypogastric nerve discharge (Fig. 7).

In additional experiments ($n = 5$) the effect of inhibition of the dorsal cMRF region on the expression of the arterial chemoreflex were analyzed. As reported above, the data show that isoguvacine microinjection into the dorsal cMRF evoked a reduction in post-inspiratory activity and iliohypogastric burst amplitude, as well as increased frequency. However, inhibiting the dorsal cMRF had little quantitative effect on the expression of arterial chemoreceptor reflex. We observed an enhanced respiratory augmentation (i.e., more PNA bursts at higher frequencies than baseline) phase of the chemoreflex following isoguvacine, with the augmentation phase T_{tot} decreasing 26 % from a control of 2.2 ± 0.3 s to 1.63 ± 0.18 s ($p = 0.03$). Plots of normalized T_{tot} that illustrate the dynamic change of respiratory frequency upon arterial chemoreceptor stimulation show that the strength of the chemoreceptor reflex relative to baseline remained unchanged. This suggests that the increased augmentation following dorsal isoguvacine was a consequence of an already elevated baseline respiratory frequency rather than an acute change in the mediation of

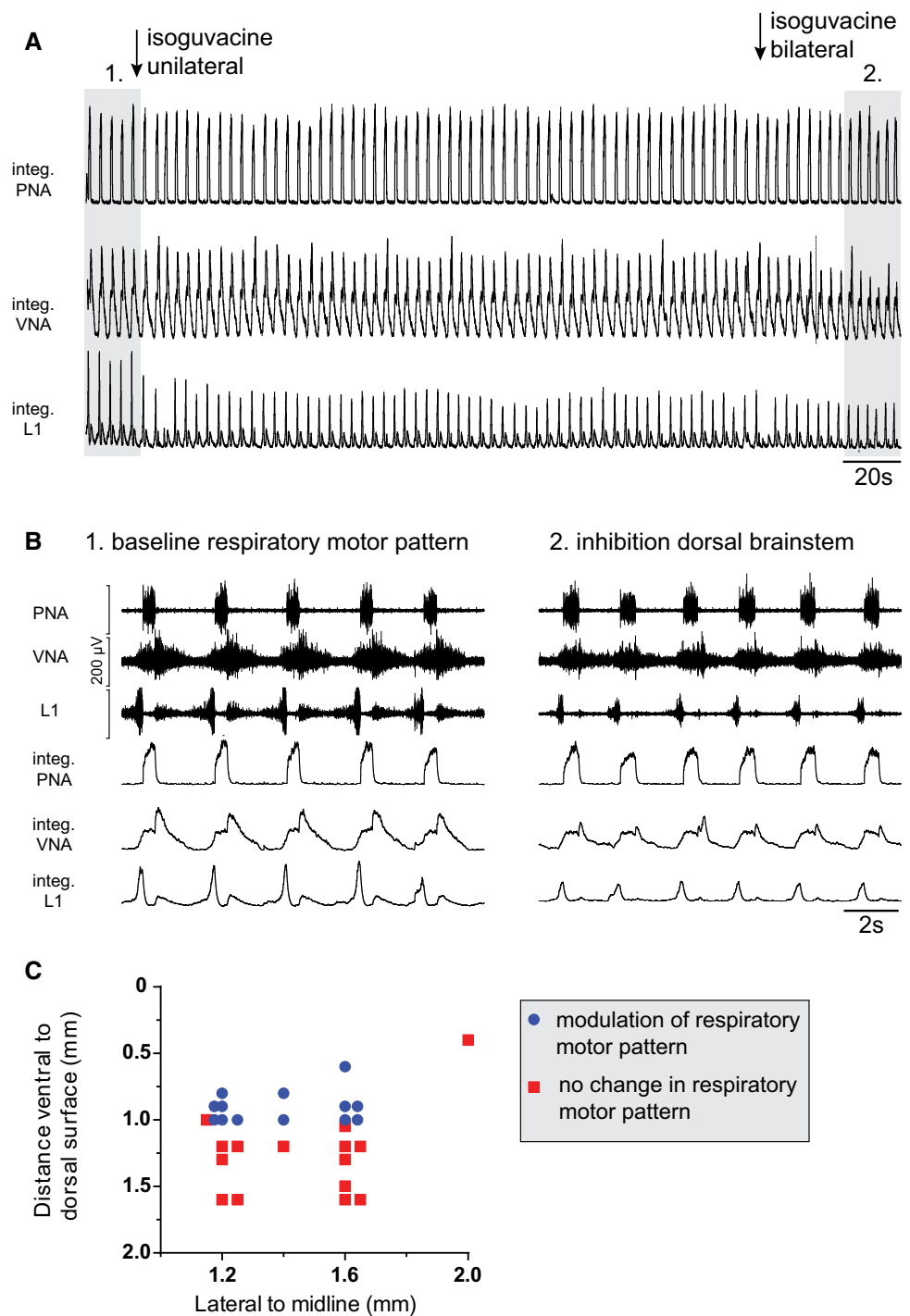
the arterial chemoreceptor reflex. The activation of abdominal expiratory activity remained unchanged during both the initial augmentation of respiratory frequency and in the post-stimulus period of enhanced expiratory abdominal activity (Fig. 8), although baseline activity was decreased, as previously reported. No significant modulation to respiratory motor pattern, or modulation of the chemoreceptor reflex was observed following isoguvacine injection into the NRA.

Discussion

Traditionally the ponto-medullary lateral respiratory column (LRC) that controls the generation of the respiratory motor pattern is thought to end approximately at the level of the obex (Alheid et al. 2004; Dutschmann and Dick 2012; Feldman et al. 2013; McCrimmon et al. 2000b; Smith et al. 1990). Nevertheless, a role for the nucleus retroambiguus (NRA) and adjacent areas of the caudal reticular formation in respiratory rhythm generation was suggested in cat (Merrill 1970; Merrill 1974) as well as in rat (Jones et al. 2012; Oku et al. 2008). In support of this view, our anterograde tracing experiments reveal robust ascending projections from the nucleus retroambiguus (NRA) within the most caudal medullary reticular formation (cMRF) to the entire ponto-medullary LRC that could serve respiratory function. Most significant terminal fields were observed in the pontine Kölliker-Fuse nucleus (KF), the parafacial respiratory group overlapping with retrotrapezoid nucleus (pFRG/RTN) and rostral and caudal ventral respiratory group (VRG). Projections to cranial motor nuclei with respiratory functions were largely restricted to the nucleus ambiguus that contains motor neurons for laryngeal valving muscles (Bartlett 1986; Iscoe et al. 1979) and facial motor neurons that innervate the nares to modulate nasal airflow resistance (Dörfl 1985).

Subsequent retrograde tracing experiments targeting the primary nuclei of the LRC that receive substantial innervation from the NRA revealed the location of dorsal and ventral clusters of ascending projection neurons within the cMRF. Our data implies that the numbers of ascending projection neurons were similar for both clusters. Chemical stimulation of both neuron clusters triggered profound modulation of the baseline respiratory motor pattern. Similar to results seen in cat, the modulation of abdominal expiratory activity recorded from the iliohypogastric nerve that innervates the abdominal musculature (e.g., oblique muscles) was particularly prominent. A novel finding of this study is that, although both clusters have the same ascending connectivity with nuclei of the LRC, only the dorsal cluster has a function in the modulation of primary respiratory motor pattern.

Fig. 7 Microinjection of isoguvacine into the dorsal but not ventral caudal medullary areas induced a significant modulation of respiratory motor pattern. **a** integrated nerve traces of Phrenic (PNA), vagus (VNA) and iliohypogastric (L1) nerves during bilateral microinjection of isoguvacine into the DRG. **b** Raw and integrated nerve traces showing increased T_i , decreased P_i and increased respiratory frequency (2) following isoguvacine injection as compared to baseline (1). **c** Dorso-ventral topography of injection sites which evoked a robust modulation of respiratory motor pattern. Note that all injections placed into the ventral cMRF overlapping the nucleus retroambiguus were ineffective

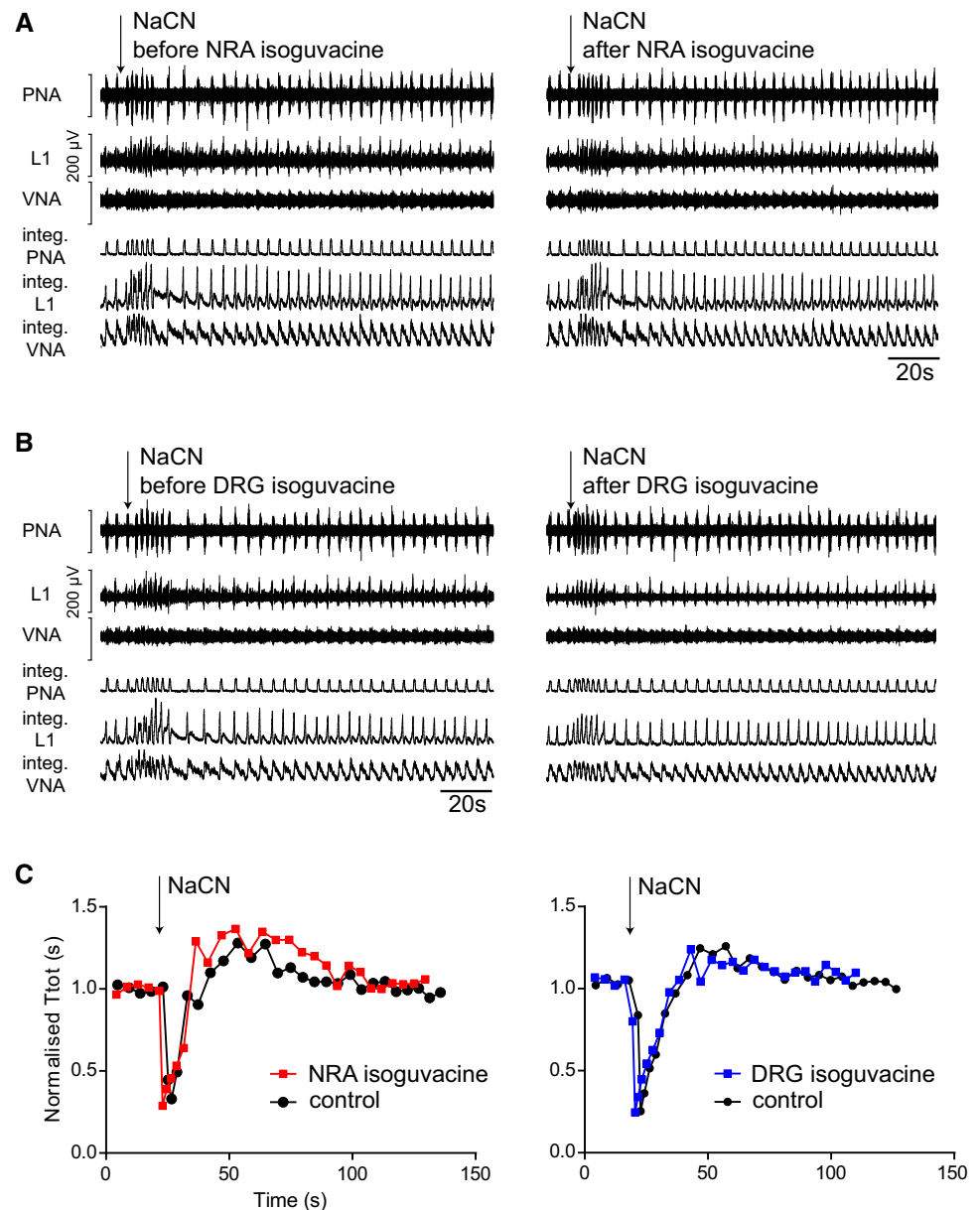


Revival of a role for the dorsal respiratory group (DRG) in the formation of the basic respiratory motor pattern

The term DRG usually refers to a population of respiratory neurons in the ventrolateral portion of NTS and was a topical research area in the 1970s and 1980s when cat was the main experimental model for studies of the neural

control of breathing. The function of the DRG was based on the presence of bulbospinal projection neurons that target the phrenic motor nucleus as a prime motor output for the vital inspiratory contraction of the diaphragm (Berger 1977; Bianchi et al. 1995; Lipski and Merrill 1980; Long and Duffin 1986). However, anatomical studies identified much smaller numbers of bulbospinal projecting DRG neurons in rat compared to bulbospinal neurons of

Fig. 8 Sodium cyanide (NaCN) evoked arterial chemoreflex response before and after inhibition of **a** nucleus retroambiguus (NRA) and **b** dorsal respiratory group (DRG) via local microinjection of isoguvacine. **c** Normalized respiratory cycle lengths (T_{tot}) for 30 bursts illustrating the NaCN evoked dynamic changes in respiratory frequencies before and after inhibition of the NRA area (red) and DRG (blue)



the ventral respiratory group (Dobbins and Feldman 1994; Yamada et al. 1988). Thus, a significant role of the DRG in the neural control of breathing in rat was lacking important anatomical substrates and its role was further questioned by lesion experiments (Hilaire et al. 1990). Subsequently, the DRG of rat received very little research focus.

A study published last year by our group put forward a role for the DRG in respiratory pattern generation in rat, based on the finding that pharmacological inhibition of the ventrolateral NTS caused a decrease in post-inspiratory motor activity and a delay in the inspiratory off-switch (Bautista and Dutschmann 2014). The study was conducted in the inter-arterially perfused brainstem preparation (Paton 1996) in which the lungs are removed and the preparation therefore

lacks any modulatory feedback from lung stretch receptors. The effects of NTS inhibition therefore cannot be attributed to the block of important regulatory reflex relays such as the Hering-Breuer reflex (for review see Kubin et al. 2006). While ascending projections of the ventrolateral NTS area into the LRC are well documented (Herbert et al. 1990; Ter Horst and Streefland 1994) the function of these projections were usually associated with the processing of viscerosensory input (see Dutschmann and Dick 2012; Kubin et al. 2006). Our results show that inhibition of caudal DRG has no qualitative effect on the expression of the arterial chemoreceptor reflex that is relayed in the neighboring commissural NTS (Zhang and Mifflin 1993), further strengthening the hypothesis that the observed effect on post-inspiration and

abdominal expiratory activity are not related to sensory relay mechanisms of the NTS.

Our previously published work together with the present study, suggest that ascending DRG projections provide the anatomical substrate for synaptic interactions that are required for the formation of the primary respiratory motor pattern. The observed changes in the synaptic drive of post-inspiratory and abdominal expiratory motor output could relate to synaptic interactions between the cMRF and the pFRG/RTN and KF nuclei. The pFRG/RTN region was identified as a key region for the generation of abdominal expiratory activity (Abdala et al. 2009; Marina et al. 2010; Molkov et al. 2010), while the KF is reported to gate the post-inspiratory activity of the respiratory pattern generator (Dutschmann and Herbert 2006; Song et al. 2012). Both pFRG/RTN and KF areas have descending projections to the cMRF with terminals innervating both the caudal DRG as well as the NRA (Krukoff et al. 1993; Rosin et al. 2006; Saper and Loewy 1980). The reciprocal connectivity between these designated key areas is a critical anatomical framework for pattern generation. However, the precise nature of pattern-related synaptic interactions needs to be further classified. Previous studies concerned with the identification of respiratory activities report respiratory single unit activities in the DRG of rat and seem to be predominantly inspiratory (Ezure et al. 1988; Saether et al. 1987). However, our findings imply a primary role of the DRG in the generation of expiratory motor activity (post-inspiration and abdominal expiration). The fact that neural activity of the DRG is reported to be predominantly inspiratory is not a discrepancy since inspiratory neurons are hypothesized to provide critical ascending synaptic drive for the pontine-mediated phase transition from inspiration to expiration [for details see (Morschel and Dutschmann 2009)]. The DRG of the caudal medulla oblongata and pontine respiratory group (e.g., the KF) in rodents form a critical network for the generation, gating and modulation of post-inspiratory laryngeal adductor function (Dutschmann et al. 2014). An important extension to this concept is that while the KF has little influence on the generation of abdominal expiratory activity (Bautista and Dutschmann 2015) the caudal DRG has a clear role in driving abdominal expiratory motor output. An important future challenge is to investigate how the DRG and KF interact to control expiratory behaviors that require the parallel activation of post-inspiratory and abdominal expiratory activity.

Respiratory functions of the nucleus retroambiguus

According to current literature, predominantly studied in cats, major afferent input to the NRA arises primarily

from the periaqueductal gray (PAG) (Gerrits and Holstege 1996; Subramanian et al. 2008; Subramanian and Holstege 2009), which functionally contributes to expulsive reflexes and behaviors (Jakus et al. 1985; Miller et al. 1990; Umezaki et al. 1997). The commonality of these behaviors is that they require the generation of intra-thoracic or abdominal pressure and modulation of the respiratory pattern. We found that glutamate stimulation of the NRA triggered qualitatively similar respiratory modulation as previously described in the cat (Subramanian and Holstege 2009). Although species differences regarding expulsive behaviors exist (e.g., rats do not vomit or cough), the general role of the NRA in modulating the basic breathing pattern and abdominal pressure seems to be the same in both species.

In cat the NRA is seen to be a relay nucleus, containing populations of pre-motor neurons that project directly into various brainstem and spinal cord motor populations, and distributing descending information from the limbic system and PAG (Holstege 2014). The descending projections from the NRA innervate motor neurons residing in the thoracic and upper lumbar ventral horn controlling expiratory intercostal muscles (Lipski and Martin-Body 1987) and abdominal muscles (Holstege 1987; Miller et al. 1987). Our data indicates that the NRA has additional ascending projections into respiratory pre-motor areas of the LRC. Sources of afferent input were not analyzed in this study, but it is likely that NRA neurons have strong reciprocal connectivity with the primary respiratory pattern generating circuitry of the LRC since descending input to the NRA has been previously reported from the parabrachial nucleus including the Kölliker-Fuse nucleus, retrotrapezoid nucleus and Bötzing complex (Gerrits and Holstege 1996).

According to our pharmacological lesion experiments, these projections appear to have no role in generation of the basic respiratory motor pattern. A recent publication from our laboratory showed the same result for the PAG. Although profound modulation of respiration can be triggered from the PAG, pharmacological inhibition had no effect on the generation of the basic breathing pattern (Farmer et al. 2014). Thus, descending limbic commands that are mediated via the PAG-NRA pathway, adapt breathing to behavior and emotion [see (Subramanian and Holstege 2014)] but this pathway apparently has no role in respiratory pattern generation.

Acknowledgments The authors' work is funded by a start-up fund from the Florey Institute of Neuroscience and Mental Health. SJ is supported by a Melbourne University International Research Scholarship. MD is supported by an ARC Future Fellowship (FT120100953). We also acknowledge the support of the Victorian Government through the Operational Infrastructure Scheme.

References

- Abdala AP, Rybak IA, Smith JC, Paton JF (2009) Abdominal expiratory activity in the rat brainstem-spinal cord in situ: patterns, origins and implications for respiratory rhythm generation. *J Physiol* 587:3539–3559
- Alheid GF, Milsom WK, McCrimmon DR (2004) Pontine influences on breathing: an overview. *Respir Physiol Neuro* 143:105–114
- Bartlett D (1986) Upper airway motor systems In: *Handbook for Physiology* ed Cherniack NS & Widdicombe JG:223–245
- Bautista TG, Dutschmann M (2014) Ponto-medullary nuclei involved in the generation of sequential pharyngeal swallowing and concomitant protective laryngeal adduction in situ. *J Physiol* 592:2605–2623
- Bautista TG, Dutschmann M (2015) The role the Kölliker-Fuse nuclei in the determination of abdominal motor output in a perfused brainstem preparation of juvenile rat. *Respir Physiol Neurobiol*. doi:10.1016/j.resp.2015.07.012
- Berger AJ (1977) Dorsal respiratory group neurons in medulla of cat—spinal projections, responses to lung-inflation and superior laryngeal nerve-stimulation. *Brain Res* 135:231–254
- Bianchi AL, Denavit-Saubie M, Champagnat J (1995) Central control of breathing in mammals—neuronal circuitry, membrane-properties, and neurotransmitters. *Physiol Rev* 75:1–45
- Boers J, Kirkwood PA, de Weerd H, Holstege G (2006) Ultrastructural evidence for direct excitatory retroambiguus projections to cutaneous trunci and abdominal external oblique muscle motoneurons in the cat. *Brain Res Bull* 68:249–256
- Borison HL, Borison R, McCarthy LE (1981) Phylogenetic and neurologic aspects of the vomiting process. *J Clin Pharmacol* 21:23S–29S
- Burke PG, Abbott SB, McMullan S, Goodchild AK, Pilowsky PM (2010) Somatostatin selectively ablates post-inspiratory activity after injection into the Botzinger complex. *Neuroscience* 167:528–539
- Cinelli E, Bongiani F, Pantaleo T, Mutolo D (2012) Modulation of the cough reflex by GABA(A) receptors in the caudal ventral respiratory group of the rabbit *Front Physiol* 3:403
- Dobbins EG, Feldman JL (1994) Brain-stem network controlling descending drive to phrenic motoneurons in rat. *J Comp Neurol* 347:64–86
- Dörfel J (1985) The innervation of the mystacial region of the white mouse: a topographical study. *J Anat* 142:173
- Dutschmann M, Dick TE (2012) Pontine mechanisms of respiratory control. *Compr Physiol* 2:2443–2469
- Dutschmann M, Herbert H (2006) The Kölliker-Fuse nucleus gates the postinspiratory phase of the respiratory cycle to control inspiratory off-switch and upper airway resistance in rat. *Eur J Neurosci* 24:1071–1084
- Dutschmann M, Mörschel M, Rybak IA, Dick TE (2009) Learning to breathe: control of the inspiratory-expiratory phase transition shifts from sensory- to central-dominated during postnatal development in rats. *J Physiol* 587:4931–4948
- Dutschmann M, Jones SE, Subramanian HH, Stanic D, Bautista TG (2014) The physiological significance of postinspiration in respiratory control. *Prog Brain Res* 212:113–130
- Ezure K, Manabe M, Yamada H (1988) Distribution of medullary respiratory neurons in the rat. *Brain Res* 455:262–270
- Farmer DG, Bautista TG, Jones SE, Stanic D, Dutschmann M (2014) The midbrain periaqueductal grey has no role in the generation of the respiratory motor pattern, but provides command function for the modulation of respiratory activity. *Respir Physiol Neurobiol* 204:14–20
- Feil K, Herbert H (1995) Topographic organization of spinal and trigeminal somatosensory pathways to the rat parabrachial and Kölliker-Fuse nuclei. *J Comp Neurol* 353:506–528
- Feldman JL, Del Negro CA, Gray PA (2013) Understanding the rhythm of breathing: so near, yet so far. *Ann Rev Physiol* 75:423–452
- Gerrits PO, Holstege G (1996) Pontine and medullary projections to the nucleus retroambiguus: a wheat germ agglutinin horseradish peroxidase and autoradiographic tracing study in the cat. *J Comp Neurol* 373:173–185
- Gestreau C, Bianchi AL, Grelot L (1997) Differential brainstem Fos-like immunoreactivity after laryngeal-induced coughing and its reduction by codeine. *J Neurosci* 17:9340–9352
- Gray PA (2013) Transcription factors define the neuroanatomical organization of the medullary reticular formation *Front Neuroanat* 7
- Guyenet P (2012) How does CO₂ activate the neurons of the retrotrapezoid nucleus? *J Physiol* 590:2183–2184
- Herbert H, Moga MM, Saper CB (1990) Connections of the parabrachial nucleus with the nucleus of the solitary tract and the medullary reticular formation in the rat. *J Comp Neurol* 293:540–580
- Hilaire G, Monteau R, Gauthier P, Rega P, Morin D (1990) Functional significance of the dorsal respiratory group in adult and newborn rats: in vivo and in vitro studies. *Neurosci Lett* 111:133–138
- Holstege G (1987) Some anatomical observations on the projections from the hypothalamus to brainstem and spinal cord: an HRP and autoradiographic tracing study in the cat. *J Comp Neurol* 260:98–126
- Holstege G (2014) The periaqueductal gray controls brainstem emotional motor systems including respiration. *Prog Brain Res* 209:379–405
- Iizuka M, Fregosi RF (2007) Influence of hypercapnic acidosis and hypoxia on abdominal expiratory nerve activity in the rat. *Respir Physiol Neurobiol* 157:196–205
- Iscoe S, Feldman JL, Cohen MI (1979) Properties of inspiratory termination by superior laryngeal and vagal-stimulation. *Respir Physiol* 36:353–366
- Jakus J, Tomori Z, Stransky A (1985) Activity of bulbar respiratory neurones during cough and other respiratory tract reflexes in cats *Physiol Bohemoslov* 34:127–136
- Janczewski WA, Feldman JL (2006) Distinct rhythm generators for inspiration and expiration in the juvenile rat. *The Journal of physiology* 570:407–420
- Janczewski WA, Onimaru H, Homma I, Feldman JL (2002) Opioid-resistant respiratory pathway from the preinspiratory neurones to abdominal muscles: in vivo and in vitro study in the newborn rat. *J Physiol-London* 545:1017–1026
- Jones SE, Saad M, Lewis DI, Subramanian HH, Dutschmann M (2012) The nucleus retroambiguus as possible site for inspiratory rhythm generation caudal to obex. *Respir Physiol Neuro* 180:305–310
- Krukoff TL, Harris KH, Jhamandas JH (1993) Efferent projections from the parabrachial nucleus demonstrated with the anterograde tracer Phaseolus vulgaris leucoagglutinin. *Brain Res Bull* 30:163–172
- Kubin L, Alheid GF, Zuperku EJ, McCrimmon DR (2006) Central pathways of pulmonary and lower airway vagal afferents. *J Appl Physiol* 101:618–627
- Lipski J, Martin-Body RL (1987) Morphological properties of respiratory intercostal motoneurons in cats as revealed by intracellular injection of horseradish peroxidase. *J Comp Neurol* 260:423–434

- Lipski J, Merrill EG (1980) Electrophysiological demonstration of the projection from expiratory neurones in rostral medulla to contralateral dorsal respiratory group. *Brain Res* 197:521–524
- Long S, Duffin J (1986) The neuronal determinants of respiratory rhythm. *Prog Neurobiol* 27:101–182
- Marina N et al (2010) Essential role of Phox2b-expressing ventrolateral brainstem neurons in the chemosensory control of inspiration and expiration. *J Neurosci* 30:12466–12473
- McCrimmon DR, Monnier A, Hayashi F, Zuperku EJ (2000a) Pattern formation and rhythm generation in the ventral respiratory group. *Clin Exp Pharmacol Physiol* 27:126–131
- McCrimmon DR, Ramirez JM, Alford S, Zuperku EJ (2000b) Unraveling the mechanism for respiratory rhythm generation. *BioEssays* 22:6–9
- Merrill EG (1970) Lateral respiratory neurones of medulla—their associations with nucleus ambiguus, nucleus retroambiguus, spinal accessory nucleus and spinal cord. *Brain Res* 24:11
- Merrill EG (1974) Finding a respiratory function for the medullary respiratory neurons. In: Bellairs, R, Gray, EG (eds) *Essays on the Nervous System Clarendon, Oxford*, 451–486
- Miller AD, Tan LK, Suzuki I (1987) Control of abdominal and expiratory intercostal muscle activity during vomiting: role of ventral respiratory group expiratory neurons. *J Neurophysiol* 57:1854–1866
- Miller A, Nonaka S, Lakos S, Tan L (1990) Diaphragmatic and external intercostal muscle control during vomiting: behavior of inspiratory bulbospinal neurons. *J Neurophysiol* 63:31–36
- Molkov YI, Abdala AP, Bacak BJ, Smith JC, Paton JF, Rybak IA (2010) Late-expiratory activity: emergence and interactions with the respiratory CpG. *J Neurophysiol* 104:2713–2729
- Monnier A, Alheid GF, McCrimmon DR (2003) Defining ventral medullary respiratory compartments with a glutamate receptor agonist in the rat. *J Physiol* 548:859–874
- Morschel M, Dutschmann M (2009) Pontine respiratory activity involved in inspiratory/expiratory phase transition. *Philos Trans R Soc Lond B Biol Sci* 364:2517–2526
- Mutolo D, Bongiani F, Cinelli E, Pantaleo T (1985) Depression of cough reflex by microinjections of antitussive agents into caudal ventral respiratory group of the rabbit. *J Appl Physiol* 109:1002–1010
- Nonaka S, Miller AD (1991) Behavior of upper cervical inspiratory propriospinal neurons during fictive vomiting. *J Neurophysiol* 65:1492–1500
- Ohi Y, Yamazaki H, Takeda R, Haji A (2004) Phrenic and iliohypogastric nerve discharges during tussigenic stimulation in paralyzed and decerebrate guinea pigs and rats. *Brain Res* 17:119–127
- Oku Y, Tanaka I, Ezure K (1994) Activity of bulbar respiratory neurons during fictive coughing and swallowing in the decerebrate cat. *J Physiol* 480:309–324
- Oku Y, Okabe A, Hayakawa T, Okada Y (2008) Respiratory neuron group in the high cervical spinal cord discovered by optical imaging. *NeuroReport* 19:1739–1743
- Olszewski JaB, D (1954) *Cytoarchitecture of the Human Brain Stem* JB Lippincott, Switzerland
- Onimaru H, Homma I (2003) A novel functional neuron group for respiratory rhythm generation in the ventral medulla. *Journal of Neuroscience* 23:1478–1486
- Paton JF (1996) A working heart-brainstem preparation of the mouse. *J Neurosci Methods* 65:63–68
- Paxinos G, Watson C (2007) *The Rat Brain in Stereotaxic Coordinates* Elsevier, San Diego 6th Ed
- Poliacek I, Wang C, Corrie LW, Rose MJ, Bolser DC (1985) Microinjection of codeine into the region of the caudal ventral respiratory column suppresses cough in anesthetized cats. *J Appl Physiol* 108:858–865
- Ramirez JM, Doi A, Garcia AJ, 3rd, Elsen FP, Koch H, Wei AD (2012) The cellular building blocks of breathing. *Compr Physiol* 2:2683–2731
- Rosin DL, Chang DA, Guyenet PG (2006) Afferent and efferent connections of the rat retrotrapezoid nucleus. *J Comp Neurol* 499:64–89
- Rybak IA, Abdala AP, Markin SN, Paton JF, Smith JC (2007) Spatial organization and state-dependent mechanisms for respiratory rhythm and pattern generation. *Prog Brain Res* 165:201–220
- Saether K, Hilaire G, Monteau R (1987) Dorsal and ventral respiratory groups of neurons in the medulla of the rat. *Brain Res* 419:87–96
- Saper CB, Loewy AD (1980) Efferent connections of the parabrachial nucleus in the rat. *Brain Res* 197:291–317
- Smith JC, Greer JJ, Liu GS, Feldman JL (1990) Neural mechanisms generating respiratory pattern in mammalian brain stem-spinal cord *in vitro*. I. spatiotemporal patterns of motor and medullary neuron activity. *J Neurophysiol* 64:1149–1169
- Smith JC, Ellenberger HH, Ballanyi K, Richter DW, Feldman JL (1991) Pre-botzinger complex—a brain-stem region that may generate respiratory rhythm in mammals. *Science* 254:726–729
- Smith JC, Abdala AP, Koizumi H, Rybak IA, Paton JF (2007) Spatial and functional architecture of the mammalian brain stem respiratory network: a hierarchy of three oscillatory mechanisms. *J Neurophysiol* 98:3370–3387
- Smith JC, Abdala AP, Rybak IA, Paton JF (2009) Structural and functional architecture of respiratory networks in the mammalian brainstem. *Philos Trans R Soc Lond B Biol Sci* 364:2577–2587
- Smith JC, Abdala AP, Borgmann A, Rybak IA, Paton JF (2013) Brainstem respiratory networks: building blocks and microcircuits. *Trends Neurosci* 36:152–162
- Song G, Wang H, Xu H, Poon CS (2012) Kolliker-Fuse neurons send collateral projections to multiple hypoxia-activated and nonactivated structures in rat brainstem and spinal cord. *Brain Struct Funct* 28:28
- Subramanian HH, Holstege G (2009) The nucleus retroambiguus control of respiration. *J Neurosci* 29:3824–3832
- Subramanian HH, Holstege G (2014) The midbrain periaqueductal gray changes the eupneic respiratory rhythm into a breathing pattern necessary for survival of the individual and of the species. *Prog Brain Res* 212:351–384
- Subramanian HH, Balnave RJ, Holstege G (2008) The midbrain periaqueductal gray control of respiration. *J Neurosci* 28:12274–12283
- Sugiyama Y, Shiba K, Nakazawa K, Suzuki T, Hisa Y (2010) Brainstem vocalization area in guinea pigs. *Neurosci Res* 66:359–365
- Ter Horst G, Streefland C (1994) Ascending projections of the solitary tract nucleus. *Nucleus of the solitary tract*:93–104
- Umezaki T, Zheng Y, Shiba K, Miller AD (1997) Role of nucleus retroambiguus in respiratory reflexes evoked by superior laryngeal and vestibular nerve afferents and in emesis. *Brain Res* 769:347–356
- Wallois F, Macron JM, Jounieaux V, Duron B (1992) Influence of trigeminal nasal afferents on bulbar respiratory neuronal activity. *Brain Res* 599:105–116
- Yamada H, Ezure K, Manabe M (1988) Efferent projections of inspiratory neurons of the ventral respiratory group. A dual labeling study in the rat. *Brain Res* 455:283–294
- Zhang W, Mifflin SW (1993) Excitatory amino acid receptors within NTS mediate arterial chemoreceptor reflexes in rats. *Am J Physiol-Heart Circul Physiol* 265:H770–H773
- Zoccal DB, Simms AE, Bonagamba LG, Braga VA, Pickering AE, Paton JF, Machado BH (2008) Increased sympathetic outflow in juvenile rats submitted to chronic intermittent hypoxia correlates with enhanced expiratory activity. *J Physiol* 586:3253–3265